Local proton dynamics in perovskite-type protonic conductors by spectral hole burning spectroscopy

S. Matsuo
Faculty of Engineering, University of Tokushima, 2-1 Minamijosanjimacho, Tokushima 770-8506, Japan

H. Yugami
Graduate School of Engineering, Tohoku University, 01 Aramaki-Aza-Aoba, Aoba-ku, Sendai 980-8579, Japan

M. Ishigame
Research Institute for Scientific Measurements, Tohoku University, Katahira 2-1-1, Aoba-ku, Sendai 980-8577, Japan
(Received 20 November 2000; published 19 June 2001)

Local proton dynamics in several kinds of perovskite-type high-temperature protonic conductors were investigated by spectral hole burning spectroscopy. Spectral holes based on light-induced protonic motion were observed. By applying a temperature-cycling technique, the potential barriers for local protonic motion, which is responsible for hole burning, were estimated. The values were several times lower than the activation energies obtained by electric conductivity measurements. The relationship between elementally protonic motion and long-range conduction mechanism is discussed based on these results.

DOI: 10.1103/PhysRevB.64.024302 PACS number(s): 78.20.−e, 66.30.Lw, 78.70.−g

I. INTRODUCTION

It is accepted that some ABO_3 perovskite-type oxides (e.g., $SrCeO_3$) show protonic conduction at high temperatures when acceptor ions are doped (strictly, a small percentage of tetravalent ions B are substituted by trivalent ions). Such protonic conduction was first discovered by Iwahara *et al*. in acceptor-doped $SrCeO_3$.[1] The electromotive force of a gas concentration cell in which acceptor-doped $SrCeO_3$ceramics were used as a diaphragm was measured, and protonic conduction was confirmed. After this discovery, a great deal of research has been carried out on protonic conduction of such materials. A group of compounds having similar crystal structures, $BaCeO_3$, $SrZrO_3$, $CaZrO_3$, $SrTiO_3$, $KTaO_3$, etc., doped with trivalent ions have also been found to show protonic conduction.[2–5]

Based on their potential applications, these materials are attracting interest because of their chemical and mechanical stability at high temperatures as well as their high protonic conductivity. Such high-temperature protonic conductors have not been found before the discovery of these materials. Thus these materials could be useful for many electrochemical applications such as high-temperature fuel cells and hydrogen sensors. In particular, $CaZrO_3$doped with the indium ion has been put to practical use as a hydrogen sensor in aluminum melts.[6]

One of the characteristic features of these perovskite-type protonic conductors is that they do not have protons as a host component; instead, protons are incorporated at the interstitial site. This is quite different from low-temperature proton conductors such as hydrate compounds and ice. Hence, for protonic conduction, it is essential that some of the Ce (Zr, Ti, Ta) ions be substituted with trivalent cations (Y, Sc, . . .). Negative-charge defects (oxygen vacancies or electron holes) are then created, and protons are incorporated as charge compensation for the defects. Incorporation of protons is carried out through an annealing process in the atmosphere, which must contain hydrogen or water vapor at high temperatures. Accordingly, it is possible to incorporate deuterons or even to remove the protons without changing the crystal structure of the host material by changing the annealing atmosphere.

Isotope effects in protonic conductivity have been observed by many researchers.[7–9] In the infrared (IR) absorption spectra, samples containing protons have a strong absorption band due to the O–H stretching vibration for both ceramic and crystalline samples.[10–12] The absorption frequency is reduced by substituting deuterons for protons. These results indicate that there is bonding between interstitial proton (or deuteron) and oxygen.

To clarify the protonic conduction mechanism from a microscopic perspective, it is important to determine the proton site in the lattice. However, it is difficult to precisely determine this site because of the low proton concentrations. Among these perovskite-type proton conductors, cerates and zirconates have relatively high proton concentrations, up to several mol %, but their crystal structure at room temperature is complicated.[13,14] In contrast, $SrTiO_3$ and $KTaO_3$ have simple cubic structures at room temperature, but their proton-absorbing feature is weaker. Thus, a precise determination of proton position is difficult. Some experimental results obtained by different experimental techniques, however, have shown some consistencies. A model in which the proton lies in one bottom of the double minimum potential between the two oxygen atoms is widely supported.[11,15] A quantum molecular dynamics simulation study of $BaCeO_3$[16] and first-principles pseudopotential calculations in Sc-doped $SrTiO_3$ (Ref. 17) are in agreement with these results.

In the present paper, we describe hole burning studies of perovskite-type protonic conductors. Using a hole burning technique, we investigated proton dynamics from a microscopic perspective. Hole burning phenomena was first reported in 1974,[18,19] and it is now recognized as a powerful technique in high-resolution spectroscopy.[20] Hereafter, the term ''hole'' will be used in the context of hole burning, that is, transient or permanent dips in an inhomogeneously broadened absorption band.

The properties of the hole reflect the nature of the host material and the optical centers. For example, the width of a hole is governed by the interaction between the optical center and low-energy excitations in the host material. Thus, hole burning can function as a sensitive probe in seeking out small structural changes around the optical center.

Many processes causing spectral hole burning have been reported, including proton tautomerization, optical pumping of the nuclear quadrupole levels, local configuration changes around the optical center, optical ionization, etc.

Hole burning due to proton (deuteron) tautomerization has been found in many organic materials. Breinl *et al.* have studied the hole burning of quinizarin in C_2H_5OH/CH_3OH (C_2D_5OD/CD_3OD) glasses, and have observed an isotope effect in the time dependence of the hole area between protonatedand deuteratedsystems.[21] In contrast to organic materials, hole burning that is related to protonic motion has been reported in only a few inorganic materials. Reeves and Macfarlane[22,23] have reported persistent spectral hole burning due to proton (deuteron) motion in the $CaF_2:Pr^{3+}:D^+$ and $SrF_2:Pr^{3+}:D^+$ system.

As reported previously, we have applied hole burning spectroscopy to the perovskite-type proton conductors, and have observed hole burning based on protonic motion.[24,25] Thus, proton dynamics can be investigated using hole burning spectroscopy. For this purpose, we have adapted the temperature-cycling experiment.[26–30]

The temperature-cycling experiment is an experimental technique that measures the distribution of the potential barrier between ground and photoproduct states. This technique was first performed by Köhler and co-workers,[28,29] and they concluded that a $V^{-1/2}$ distribution exists in tetracene-doped alcohol glass. Kurita *et al.* have applied this technique to free-base myoglobin, concluding that the relaxation of holes is governed by the rotation of inner protons.[30] In cases where hole burning is based on ionic motion, the potential barrier estimated from this experiment seems to correspond to the potential barrier of an ion hopping from one site to another. Hence, the potential barrier of specific ion hopping can be estimated by this method.

II. EXPERIMENTS

A. Samples

Samples were single crystals of $SrZrO_3$, $SrCeO_3$, or $SrTiO_3$ in which some of the Zr, Ce, or Ti was substituted with trivalent ions (Y, Sc), as summarized in Table I. There was slight doping with Pr^{3+} ions to serve as optical centers for hole burning. The samples were made by the floating-zone method, as described previously.[25,10] After optical polishing, the samples were annealed in an adequate atmosphere to obtain (1) protonated (containing protons), (2) deuterated (containing deuterons), and (3) dry (containing neither protons nor deuterons) states. Incorporation of protons (deuterons) was examined by measuring the absorption intensity of the O–H (O–D) stretching band by IR spectroscopy. Since $SrCeO_3$(Y:5) is very hygroscopic, protons were incorporated into the sample during the crystal growth process and could not be removed completely by postannealing in a dry atmosphere. For this reason, only protonated and deuterated samples were obtained for the $SrCeO_3$(Y:5) crystals. In contrast, protonated, deuterated, and dried samples were obtained for $SrZrO_3$ crystals. Exceptionally, only dried samples were obtained for $SrZrO_3$(Pr:5). Because the $SrTiO_3$(Sc:5) crystals were less hygroscopic, dried $SrTiO_3$(Sc:5) was easily obtained. However, $SrTiO_3$(Sc:5) showed only a weak O–H stretching mode after the annealing in water vapor under atmospheric pressure. As such, the $SrTiO_3$(Sc:5) crystals used in this study were annealed at high-pressure (approximately 15 atm) water-vapor atmosphere. After this annealing, the absorption intensity of the O–H mode of $SrTiO_3$(Sc:5) crystals was comparable to that of protonated $SrZrO_3$(Y:5).

TABLE I. Samples used in the present study.

Sample name	Content
$SrZrO_3$(Y:5)	$SrZr_{0.95}Y_{0.049}Pr_{0.001}O_3$
$SrZrO_3$(Sc:5)	$SrZr_{0.95}Y_{0.049}Pr_{0.001}O_3$
$SrZrO_3$(Y:10)	$SrZr_{0.9}Y_{0.099}Pr_{0.001}O_3$
$SrZrO_3$(Pr:5)	$SrZr_{0.95}Pr_{0.05}O_3$
$SrCeO_3$(Y:5)	$SrCe_{0.95}Y_{0.04}Pr_{0.01}O_3$
$SrTiO_3$(Sc:5)	$SrTi_{0.95}Y_{0.04}Pr_{0.01}O_3$

B. Hole burning

The experimental setup for the hole burning study has been described previously.[24,25] The samples were placed in a cryostat (Oxford Instruments CF-1204) controlled by a temperature controller (Oxford Instruments CF-1240). A single-mode scanning ring dye laser (COHERENT 899-21) operating with Rhodamine 6G was used as light source. The ring laser was used because of its tunability and its narrow linewidth (the nominal linewidth is 1 MHz). Holes were burned by exciting the $^3H_4$-$^1D_2$ zero-phonon transition at a single frequency around 605–610 nm, and hole spectra (excitation spectra) were measured by sweeping a laser monitoring luminescence around 620–630 nm.

The procedure for the temperature-cycling experiment was as follows.

(1) A hole was burned at a low temperature, T_b. In the present study, T_b was set to 6 K or 10 K. The results showed no dependence on T_b.

(2) After approximately an hour, the hole spectrum was measured.

(3) The sample temperature was increased to T, which is referred to as the ''excursion temperature'' or ''cycling temperature.''

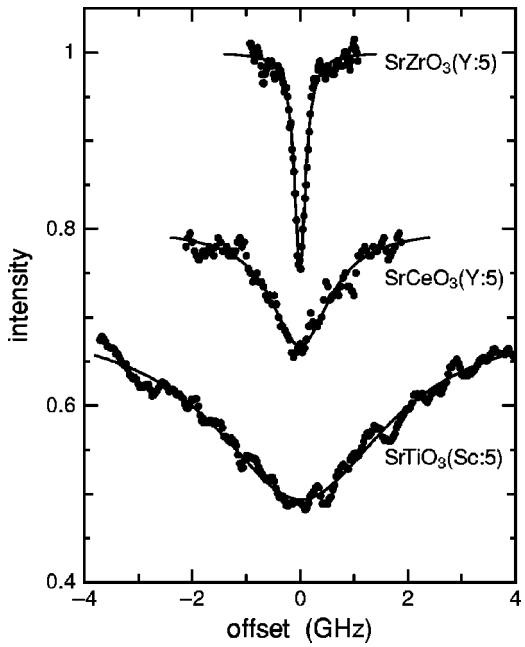

FIG. 1. Hole spectra of $SrZrO_3$(Y:5), $SrCeO_3$(Y:5), and $SrTiO_3$(Sc:5). All of them are protonated. Solid curves are the fitted ones by a Lorentzian. Burning power and time, and measured temperatures are: $SrZrO_3$(Y:5); 1 mW$\times$840 sec at 6 K, $SrCeO_3$(Y:5); 1 mW$\times$900 sec at 10 K, $SrTiO_3$(Sc:5); 40 mW $\times$1200 sec at 6 K.

(4) The sample temperature was kept at T for a period τ, 2 min in this study, and then cooled to T_b.

(5) The hole spectrum was measured again.

(6) Steps (3)–(5) were carried out repeatedly with increasing T. Hole spectra were recorded and analyzed as a function of T.

From this experiment, the excursion temperature dependence of the hole area $A(T)$ was obtained, and distribution of the potential barrier height $P(V)$ was estimated. The relation between $A(T)$ and $P(V)$ is written as

$$\frac{A(T)}{A(T_b)} = \int_{kT\ln(R_0\tau)}^{\infty} P(V)dV, \tag{1}$$

where $A(T_b)$ is the initial hole area at T_b, and R_0 is the attempt frequency. From this equation, we can estimate $P(V)$. It should be stressed that the change in R_0 does not affect the factor of $\ln(R_0\tau)$ significantly, although the estimation of R_0 is difficult and it may cause an error in calculating the potential barrier.[28] In the analysis, we supposed that the value of R_0 is on the order of the O–H stretching frequency, so that the value of $\ln(R_0\tau)$ was 35. The error for the absolute value of $\ln(R_0\tau)$ will be within $\pm$30%, and relatively within $\pm$10% among the samples used in this study.

III. RESULTS AND DISCUSSION

Figure 1 shows typical hole spectra of three protonated materials. While holes can be burned in all of these materials, the bandwidths of the spectra are different among the three samples. For example, the bandwidth of the hole measured on $SrCeO_3$(Y:5) was approximately about five times larger than that measured on $SrZrO_3$(Y:5). This difference may be ascribed in part to the different burning parameters.

TABLE II. Hole burning properties of the samples. ○, holes were burned; ×, holes were not burned; –, not tested.

Sample name	Protonated	Deuterated	Dry
$SrZrO_3$(Y:5)	○	○	×
$SrZrO_3$(Sc:5)	○	○	×
$SrZrO_3$(Y:10)	○	–	–
$SrZrO_3$(Pr:5)	–	–	×
$SrCeO_3$(Y:5)	○	–	–
$SrTiO_3$(Sc:5)	○	–	×

In order to examine the relation between hole burning phenomena and absorbed protons or deuterons, hole burning experiments were performed on various protonated, deuterated, and dried samples. The results are summarized in Table II. The relation is obvious. Holes were burned on all protonated and deuterated samples, but were not burned on all dried samples. These results indicate that protons (deuterons) are responsible for the hole burning phenomena.

Figure 2 shows hole spectra of protonated (lower) and deuterated (upper) $SrZrO_3$(Y:5) burned with the same parameters. The line shape of the hole spectrum of the protonated sample seems to be almost identical to that of the deuterated sample. However, the hole depths (or hole burning rates) are clearly different among them. The burning rate of the deuterated samples were very small compared with that of the protonated sample. Such an isotope effect on the burning rate has been observed in organic materials[29] and fluorides.[31] In such cases, the origins of the hole burning have been assigned to protonic motion.

The shape of spectral holes is given by a Lorentzian (Fig. 1), which is characteristic of hole burning caused by a local configuration change around the optical center. Such hole burning has been observed in Pr^{3+}-doped samples.[32,33]

The temporal change in hole spectra has been measured,

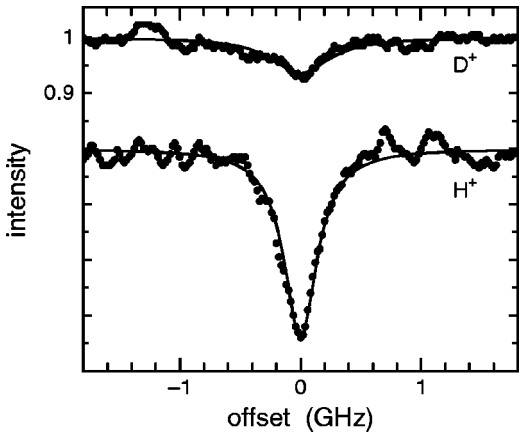

FIG. 2. Hole spectra of $SrZrO_3$(Y:5) measured at 6 K. The upper spectrum was obtained from a deuterated sample, and the lower from a protonated sample. Burning power and time are identical (10 mW$\times$240 sec). Solid curves are the fitted curves.

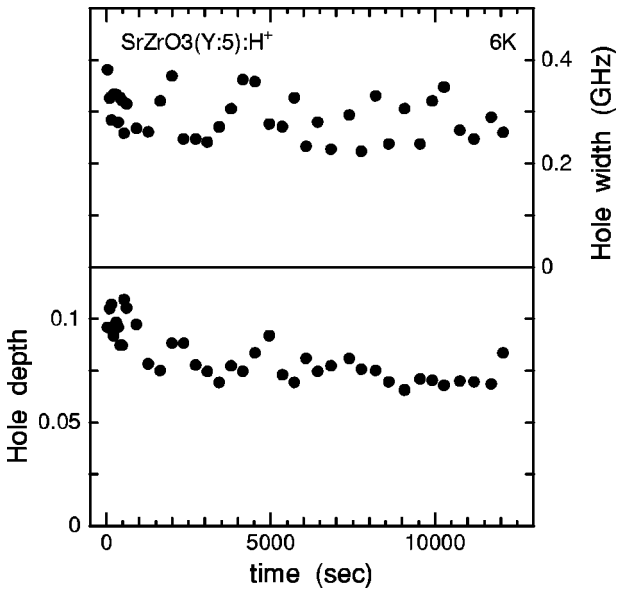

FIG. 3. Time dependence of hole width (upper panel) and hole area (lower panel) of protonated $SrZrO_3$(Y:5) measured at 6 K.

and Fig. 3 shows the time dependence of the hole area and hole width of protonated $SrZrO_3$(Y:5) at 6 K. As shown in the figure, more than half of the hole area remains at 10^4 sec. Such a long, almost persistent lifetime is also characteristic of hole burning caused by a local configurational change around the optical center.

These results described above were commonly observed for all samples. Hence, we conclude that the hole burning observed in these materials is based on proton motion near an optical center (Pr^{3+} ion).

If the hole burning in these perovskite-type oxides is related to light-induced protonic motion, the barrier height between metastable and ground states for protons can be connected to the activation energy of local structural change accompanying protonic motion. To investigate such ''microscopic'' barrier heights, we carried out a temperature-cycling experiment.

Figure 4 shows the change in hole spectra through temperature-cycling in $SrZrO_3$(Sc:5). As can be seen, the depth of the hole decreased with increasing excursion temperatures, while the width did not change significantly. From the spectra of each excursion temperature, the excursion temperature dependence of the hole areas was obtained. In the present case, the temperature dependence was well fitted by a model assuming a Gaussian-type distribution of potential barrier heights,[30,27] i.e.,

$$P(V) \propto \exp[-(V-V_0)^2/2\sigma_V^2], \tag{2}$$

where V_0 and σ_V are the central value and width of the distribution, respectively. The excursion temperature dependence of the hole area is then represented as

$$\frac{A(T)}{A(T_b)} = \frac{1-\mathrm{erf}[(T-T_0)/\sqrt{2}\sigma_T]}{1-\mathrm{erf}[(T_b-T_0)/\sqrt{2}\sigma_T]}, \tag{3}$$

where $T_0 = V_0/k\ln(R_0\tau)$, and $\sigma_T = \sigma_V/k\ln(R_0\tau)$. Figure 5

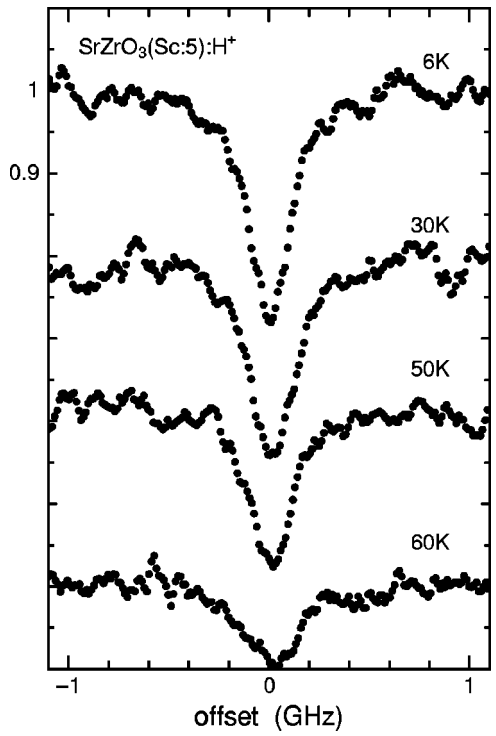

FIG. 4. Hole spectra of protonated $SrZrO_3$(Sc:5)at several excursion temperatures. The hole was burned and the spectra were measured at 6 K.

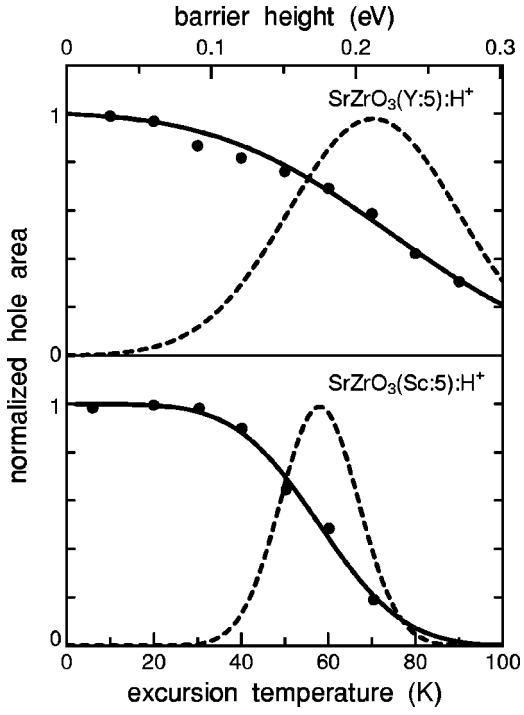

FIG. 5. Excursion temperature dependence of the hole area for $SrZrO_3$ with two different acceptors. Solid circles represent experimental values. The fitted curves (solid curves), and the distribution of the potential barrier height (broken curves, top axis) were obtained by using Eqs. (2) and (3).

TABLE III. The values of V_0 and σ_V, obtained by temperature-cycling experiment, and ΔE, obtained by electric conductivity measurement.

	Hole burning		Electric conductivity
	V_0	σ_V	ΔE
Sample	(eV)	(eV)	(eV)
$SrZrO_3(Y:5):H^+$	0.22	0.10	0.56
$SrZrO_3(Y:5):D^+$	0.22	0.09	
$SrZrO_3(Sc:5):H^+$	0.18	0.05	0.59
$SrZrO_3(Sc:5):D^+$	0.17	0.06	
$SrZrO_3(Y:10):H^+$	0.22	0.10	
$SrCeO_3(Y:5):H^+$	0.26	0.09	0.61
$SrTiO_3(Sc:5):H^+$	0.11	0.07	0.46

shows the excursion temperature dependence of the hole area and the fitted curves, and the Gaussian distribution of barrier heights for protonated $SrZrO_3$(Y:5) and $SrZrO_3$(Sc:5).

The obtained values of V_0 and σ_V are summarized in Table III. For comparison, we have also measured the electric conductivity for protonated samples and obtained the activation energy (ΔE) from its temperature dependence. The results are also shown in Table III. As seen in the table, the barrier height and its distribution width estimated by temperature cycling depended on acceptor ions in the $SrZrO_3$ host material. $SrZrO_3$(Y:5) showed a higher barrier and broader distribution compared with $SrZrO_3$(Sc:5). These differences may be related to the difference in the O–H bonding state between these systems. In Fig. 6, which shows the IR spectra of $SrZrO_3(Y:5):H^+$ and $SrZrO_3(Sc:5):H^+$ measured at room temperature, two differences can be seen between the samples.

(i) The average absorption frequency in $SrZrO_3$(Sc:5)is higher than that in $SrZrO_3$(Y:5).

(ii) The distribution of absorption frequency in $SrZrO_3$(Sc:5) is narrower than that in $SrZrO_3$(Y:5).

The result (ii) will be related to the difference in σ_V, which was smaller in $SrZrO_3$(Sc:5) than in $SrZrO_3$(Y:5).

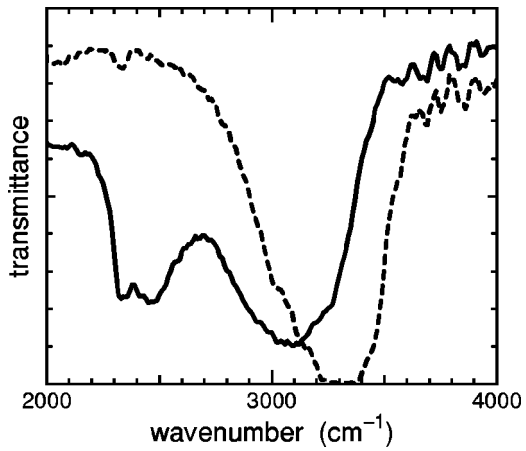

FIG. 6. IR spectra of $SrZrO_3(Y:5):H^+$ (solid curve) and $SrZrO_3(Sc:5):H^+$ (broken curve). The dip around 2300 cm^{-1} is due to the absorption of CO_2 that was not removed completely.

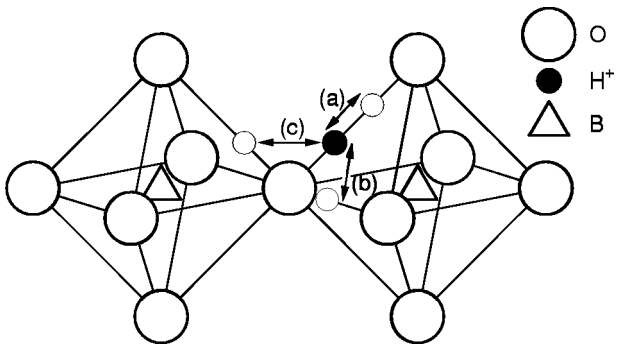

FIG. 7. Elementary protonic motions in an ABO_3-type perovskite structure.

The result (i), which is more important, shows that the bonding between O and H in $SrZrO_3$(Sc:5)is stronger than that in $SrZrO_3$(Y:5). In addition, the potential barrier height in $SrZrO_3$(Sc:5) as observed by the temperature-cycling experiment is lower than that in $SrZrO_3$(Y:5), indicating that the protonic motion that induces hole burning retains the bonding between O and H.

As seen in Table III, the potential barrier (V_0) obtained by hole burning is several times lower than the activation energies (ΔE) obtained from electric conductivity measurements. It can therefore be concluded that the protonic motion observed by hole burning is different from the rate-determining process for electric conduction.

In these perovskite-type proton conductors, there are three types of elementary protonic motion, as shown in Fig. 7. These types can be classified into two categories from the perspective of O–H bonding. The motion (a) breaks the bonding between the oxygen and the proton, while in (b) and (c) the proton rotates around an oxygen and retains the bonding with the oxygen. For the long-range diffusion of protons, all three types of protonic motion are required. Thus the slowest motion limits the mobility of proton diffusion.

As described above, the strength of bonding between O and H in $SrZrO_3$(Sc:5) is stronger than that in $SrZrO_3$(Y:5). In contrast, ΔE in $SrZrO_3$(Y:5) is higher than that in $SrZrO_3$(Sc:5), suggesting that long-range diffusion of protons is limited by process (a) in Fig 7. This finding is also supported by the relation between the O–O distance and ΔE. Among the materials used, the longer the O–O distance, the higher is ΔE. In addition, the obtained values of ΔE are close to the calculated barrier height between the double minimum in the O–O bonding.[34,35] Quantum molecular dynamics studies have shown that path (a) has the highest potential for proton diffusion,[16,36] which is also consistent with our results.

IV. CONCLUSION

Persistent hole burning due to photo-induced local protonic motion was observed in Pr^{3+} -doped perovskite-type protonic conductors. From the temperature-cycling experi-

ment, the activation energies of this type of proton motion were estimated. The obtained values for the activation energies were several times lower than those obtained by electric conductivity. It was found that the protonic motion accompanying hole burning retains the bonding between the proton and oxygen, and the rate-determining process for protonic conduction is a motion that breaks these bonds.

ACKNOWLEDGMENTS

The authors are grateful to Professor T. Hattori at Tohoku University for useful discussion. This work was supported in part by a Grant-in-Aid for Scientific Research on Priority Areas (A) (Grant No.10148106), and Scientific Research (B) (Grant No. 12450262).

[1] H. Iwahara, T. Esaka, H. Uchida, and N. Maeda, Solid State Ionics **3/4**, 359 (1981).
[2] H. Iwahara, in *Proton Conductors*, edited by P. Colomban (Cambridge University Press, New York, 1992), pp. 122–137.
[3] A.S. Nowick and Y. Du, Solid State Ionics **77**, 137 (1995).
[4] K.D. Kreuer, Chem. Mater. **8**, 610 (1996).
[5] K.D. Kreuer, Solid State Ionics **125**, 285 (1999).
[6] T. Yajima, K. Koide, N. Fukatsu, T. Ohashi, and H. Iwahara, Sens. Actuators B **13-14**, 697 (1993).
[7] T. Scherban and A.S. Nowick, Solid State Ionics **35**, 189 (1989).
[8] H. Huang, M. Ishigame, and S. Shin, Solid State Ionics **47**, 251 (1991).
[9] J.F. Liu and A.S. Nowick, Solid State Ionics **50**, 131 (1992).
[10] S. Shin, H.H. Huang, M. Ishigame, and H. Iwahara, Solid State Ionics **40/41**, 910 (1990).
[11] G. Weber, S. Kapphan, and M. Wöhlecke, Phys. Rev. B **34**, 8406 (1986).
[12] T. Hibino, K. Mizutani, T. Yajima, and H. Iwahara, Solid State Ionics **58**, 85 (1992).
[13] M. Ahtee, A.M. Glazer, and A.W. Hewat, Acta Crystallogr., Sect. B: Struct. Crystallogr. Cryst. Chem. **34**, 752 (1978).
[14] A. Saeki, H. Seto, H. Seki, N. Ishizawa, S. Kato, and N. Mizutani, Nippon Kagaku Kaishi **1991**, 25 (1991).
[15] N. Sata, K. Hiramoto, M. Ishigame, S. Hosoya, N. Niimura, and S. Shin, Phys. Rev. B **54**, 15 795 (1996).
[16] W. Münch, G. Seifert, K.D. Kreuer, and J. Maier, Solid State Ionics **86-88**, 647 (1996).
[17] F. Shimojo, K. Hoshino, and H. Okazaki, J. Phys. Soc. Jpn. **65**, 1143 (1996).
[18] B.M. Kharlamov, R.I. Personov, and L.A. Bykovskaya, Opt. Commun. **12**, 191 (1974).
[19] A.A. Gorokhovskii, R. Kaarli, and L.A. Rebane, Pis'ma Zh. Éksp. Teor. Fiz. **20**, 474 (1974) [JETP Lett. **20**, 216 (1974)].
[20] *Persistent Spectral Hole-Burning: Science and Applications*, edited by W. E. Moerner (Springer-Verlag, Berlin, 1988).
[21] W. Breinl, J. Friedrich, and D. Haarer, Chem. Phys. Lett. **106**, 487 (1984).
[22] R.J. Reeves and R.M. Macfarlane, Phys. Rev. B **47**, 158 (1993).
[23] R.J. Reeves and R.M. Macfarlane, J. Opt. Soc. Am. B **9**, 763 (1992).
[24] S. Matsuo, H. Yugami, M. Ishigame, and S. Shin, J. Lumin. **64**, 267 (1995).
[25] H. Yugami, S. Matsuo, and M. Ishigame, Solid State Ionics **77**, 195 (1995).
[26] B. Sauter and C. Bräuchle, J. Lumin. **56**, 117 (1993).
[27] P. Schellenberg, J. Friedrich, and J. Kikas, J. Chem. Phys. **101**, 9262 (1994).
[28] W. Köhler and J. Friedrich, Phys. Rev. Lett. **59**, 2199 (1987).
[29] W. Köhler, J. Meiler, and J. Friedrich, Phys. Rev. B **35**, 4031 (1987).
[30] A. Kurita, R. Ohmukai, and T. Kushida, J. Lumin. **53**, 255 (1992).
[31] R.M. Macfarlane, R.J. Reeves, and G.D. Jones, Opt. Lett. **12**, 660 (1987).
[32] R.M. Macfarlane and R.M. Shelby, in *Persistent Spectral Hole-Burning: Science and Applications*, edited by W.E. Moerner (Springer-Verlag, Berlin, 1988), pp. 127–151.
[33] T. Okuno and T. Suemoto, Phys. Rev. B **59**, 9078 (1999).
[34] E. Matsushita and T. Sasaki, Solid State Ionics **125**, 31 (1999).
[35] S. Scheiner, in *Proton Transfer in Hydrogen-Bonded Systems*, edited by T. Bountis (Plenum Press, New York, 1992), pp. 29–47.
[36] W. Münch, G. Seifert, K.D. Kreuer, and J. Maier, Solid State Ionics **97**, 39 (1997).